CHEMISTRY
A EUROPEAN JOURNAL

DOI: 10.1002/chem.200500830

Polyelectrolyte Templated Polymerization in Langmuir Films: Nanoscopic Control of Polymer Chain Organization

M. Sharath Chandra and T. P. Radhakrishnan*[a]

Abstract: Polyelectrolytes introduced in the aqueous subphase are shown to have a profound impact on the kinetics of polymerization of *N*-octadecylaniline at the air/water interface. This can be attributed to changes effected in molecular organization and reorientation behavior in the Langmuir film. The polyelectrolyte templates lead to considerable modification of the morphology of the monomer and polymer Langmuir films. Polyelectrolyte complexation is found to be an elegant and efficient methodology to achieve enhanced alignment of the polyaniline chains in the transferred Langmuir–Blodgett (Langmuir–Schafer) film.

Keywords: interfaces · Langmuir films · polyaniline · polyelectrolytes · polymerization · template synthesis

Introduction

Molecular assembly mediated by covalent and noncovalent interactions and its control at the nanoscopic level are of fundamental relevance to supramolecular chemistry, polymer chemistry, and molecular-scale electronics, photonics, and patterning. The Langmuir–Blodgett (LB) technique is especially suited to exercise such control; this technique also facilitates efficient monitoring of the assembly process. A fine example is the synthesis of conjugated polymers at the air/water interface[1,2] and investigation of the kinetics through the measurement of surface-pressure/monolayer-area changes.[1,3–6] We have previously demonstrated the utility of polyelectrolyte complexation in stabilizing otherwise unstable Langmuir films[7] and the role of polyelectrolyte templates in efficient deaggregation leading to enhanced[8] and stable[9] second-harmonic generation in LB films of hemicyanines. Polyelectrolytes have been extensively employed as dopants and templates in the synthesis of conducting polymers;[10,11] they impart higher solubility and processability to the polymers and modify the morphology and conducting properties.[11] Polyion-complexed diacetylene has been photopolymerized following LB film deposition.[12] A logical extension of the studies cited above suggests that the covalent assembly of molecules through polymerization at the air/water interface, modulated by noncovalent interactions with polyelectrolytes introduced in the subphase, could be an efficient approach to the controlled organization of polymers in ultrathin films.

We have chosen to investigate the polymerization of *N*-octadecylaniline (NOA) assembled as a Langmuir film on the surface of water and demonstrate the influence of polyelectrolytes introduced from the subphase on the morphology of the Langmuir film, rates of polymerization, and the polymer-chain organization in the transferred Langmuir–Schafer film. Polymerized *N*-alkylaniline cannot sustain the conventional emeraldine base (neutral quinonoid) and the corresponding salt (protonated) forms because of the substitution on the nitrogen atom. Polymers with alkyl groups, butyl to dodecyl, synthesized in the bulk phase were found to exhibit low conductivity.[13] However, NOA possesses the advantages of easy synthesis, stable protonated monomer/polymer states, and steric/structural features conducive for organization at the air/water interface; therefore it should serve as a suitable candidate to demonstrate phenomena associated with the molecular assembly and reaction. We envisaged that, under the usual aniline polymerization conditions, polyelectrolytes would exercise strong control on the orientation of the protonated monomer and the organization of the polymer, which is likely to form in the fully protonated (with ammonium groups) or further oxidized (bipolaronic) form. Brewster angle microscopy (BAM) was employed to observe the monolayer at the air/water interface through the polymerization process and investigate the in-

[a] M. S. Chandra, Prof. T. P. Radhakrishnan
School of Chemistry, University of Hyderabad
Hyderabad, 500 046 (India)
Fax: (+91) 40-2301-2460
E-mail: tprsc@uohyd.ernet.in

Supporting information for this article is available on the WWW under http://www.chemeurj.org/ or from the author.

fluence of the polyelectrolytes in the subphase on the domain morphologies. A new protocol that we have developed facilitated accurate monitoring of the rates of polymerization at the air/water interface and the impact of the polyelectrolytes. Atomic force microscopy (AFM) images of the transferred Langmuir–Schafer films revealed the utility of polyelectrolyte templating in directing the formation of organized chains of poly(*N*-octadecylaniline) in these films.

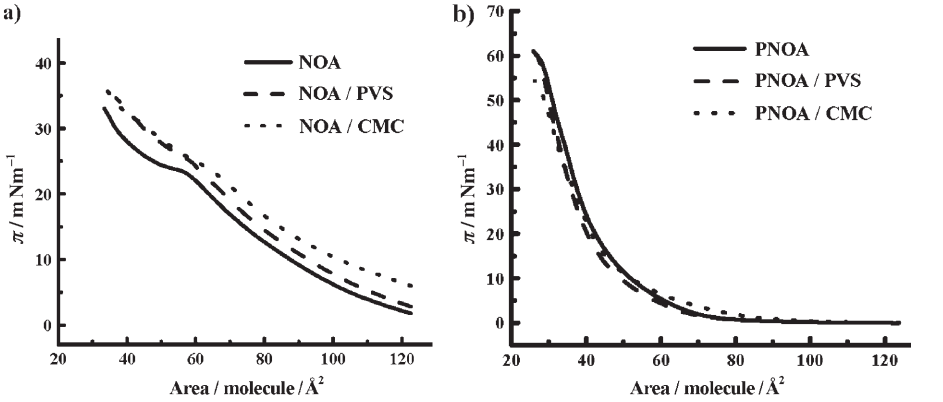

Figure 1. Pressure–area (π vs. A) isotherms of protonated a) NOA and b) PNOA monolayers without and with polyelectrolytes in the subphase; note the different y scales.

Results and Discussion

NOA was synthesized by the reaction of 1-bromooctadecane with aniline (Scheme 1). It does not show any tendency to spread evenly and form a monolayer on the surface of pure water. Acidification of the subphase with hydrochloric acid facilitated spreading; however, the monolayer was found to be unstable to compression. Interestingly, introduction of sulfuric acid in the subphase imparted appreciable stability to the monolayer as revealed by the pressure–area isotherm and the collapse pressure of ~33 mN m^{-1} (Figure 1a). It appears that the protonated NOA layer is stabilized by the bidentate dianion; this stabilization is reminiscent of earlier observations on pyridinium-based amphiphiles.[7,8] The isotherm shows a transition at ~23 mN m^{-1}; based on the extrapolated areas below and above, 101.6 and 75.8 Å^2 per molecule, respectively, the transition can be ascribed to a reorientation of the headgroup.[14,15] The polyelectrolytes used in this study are the salts of poly(vinylsulfate) (PVS) and carboxymethylcellulose (CMC); they are likely to be mostly in the polyacid form under the acidic conditions employed in this work. Introduction of polyelectrolytes in the subphase increased the residual pressure slightly, but more significantly it shifted the isotherms to higher areas and smoothed the transition. The extrapolated areas above the transition are 96.7 and 94.1 Å^2 per molecule with PVS and CMC, respectively. The increase of residual pressure possibly arises as a result of the adsorption of the polyelectrolyte at the air/water interface by the amphiphile monolayer and the isotherm shift is a consequence of the amphiphile–polyelectrolyte complexation.[7–9] The complexation also effects a cooperative motion of the headgroups leading to a smoothening of the transition. A combination of electrostatic and hydrogen-bonding interactions, depending on the level of ionization of the polyacids, is likely to lead to the complexation.

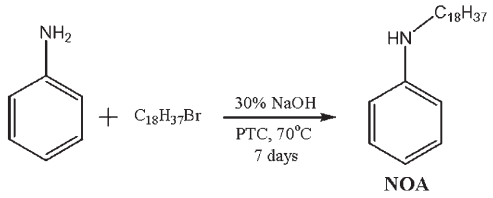

Scheme 1.

Previous studies of polymerization of anilines at the air/water interface involved spreading the monolayer on a subphase already charged with the oxidizing agent.[3–5] We have investigated the polymerization of NOA using such a procedure.[16] However, we found that the kinetics is affected by the barrier speed and delays in the initial compression; hence, a new protocol was developed (Scheme 2). The monomer was spread on the acidic subphase and compressed to the desired pressure. Subsequently, the oxidizing agent (ammonium peroxydisulfate as aqueous solution) was injected into the subphase with a surgical needle inserted through the monolayer; this had no adverse effect on the film. In this procedure, the monomers are organized before initiat-

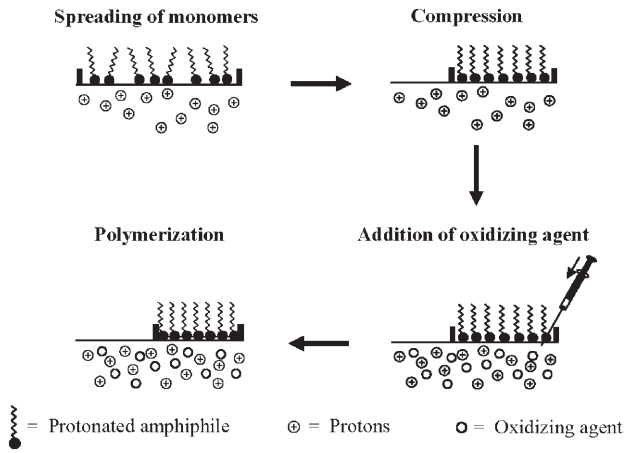

Scheme 2.

ing the polymerization and the rate is monitored from the start; conceptually it is similar to the double-compartment method reported previously.[6] Reactions were carried out at 25 °C with constant target pressures of 20, ~23 and 30 mN m^{-1} (below, near, and above the transition). The rate of the reaction at the interface can be formulated within the spirit of the 2D "ideal-gas equation" [Eq. (1)], in which π, A, and n are the surface pressure, area, and number of monomers during the course of the reaction. A_∞ is the final area and C is a constant.

$$\pi(A-A_\infty) = Cn \quad (1)$$

At constant temperature, the rate is given by Equation (2),[16] in which π_0, A_0, and n_0 are the initial values.

$$\text{Rate} = \frac{n_0}{\pi_0(A_0-A_\infty)}\frac{\mathrm{d}}{\mathrm{d}t}[\pi(A_\infty-A)] \quad (2)$$

This expression takes into account possible minor pressure fluctuations ($\pi \sim \pi_0$) in the "constant-pressure" experiment. The rates were determined by following the change of the monolayer area with time at a constant target pressure and employing the above equation at each point (Figure 2). The rate varies through the reaction; the peak rates obtained for NOA polymerization carried out at different target pressures, with and without the polyelectrolytes in the subphase are summarized in Table 1. Without polyelectrolytes, the peak rate is highest near the transition, indicating that the reaction is aided by the molecular reorientation at this point. Significantly, the polyelectrolytes reduce the rates in general and the peak rate decreases with increasing pressure. These observations point to the control of monomer motion and reorientation by the cooperative impact of the polyelectrolyte.

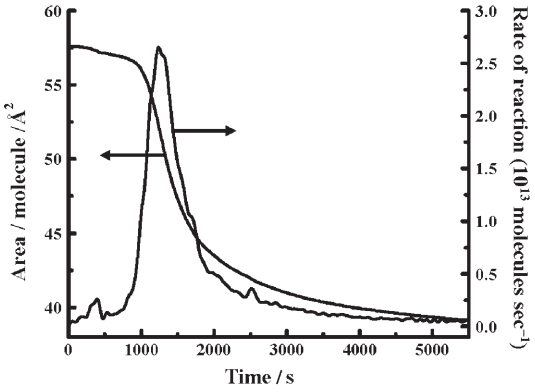

Figure 2. Change of monolayer area and rate of reaction with time during the polymerization of NOA (sulfate in subphase, target pressure = 25 mN m^{-1}); zero on the time axis indicates the point when the oxidizing agent was injected in.

Table 1. Peak rate of polymerization of NOA at 25 °C with only sulfate and with different polyelectrolytes in the subphase.

Pressure [mN m^{-1}]	Rate [10^{13} molecules s^{-1}]		
	Sulfate	PVS	CMC
20	2.24	1.66	1.40
~23	2.61	1.30	1.15
30	1.40	1.06	0.89

The π versus A isotherms of poly(*N*-*n*-octadecylaniline) (PNOA) (Figure 1b) show steeper curves, higher collapse pressures, and lower extrapolated areas (~40 Å^2 per molecule), relative to those of the monomer. The contraction of area results from covalent-bond formation. The steeper curves and higher collapse pressures reveal the enhanced stiffness and stability of the polymer monolayer. Interestingly, the isotherms are nearly independent of the presence or type of polyelectrolyte, indicating that polyaniline backbones are identical in all cases. BAM of the monolayer at different points along the π versus A curve, through the polymerization process, reveals the influence of the polyelectrolytes. Images for the polymerization carried out at 20 mN m^{-1} are presented in Figure 3. The polyelectrolytes support domain formation prior to polymerization (panel 1). The change of morphology on polymerization (panels 2 and 3) is marked in the absence of polyelectrolytes; the polyelectrolytes homogenize the monomer and polymer monolayers smearing out contrast. The most significant impact of the polyelectrolytes is evident upon expansion of the polymer monolayer (panel 4). The entangled network structures present in the case of PNOA give way to short broken chainlike features when polyelectrolytes are present in the subphase during polymerization.

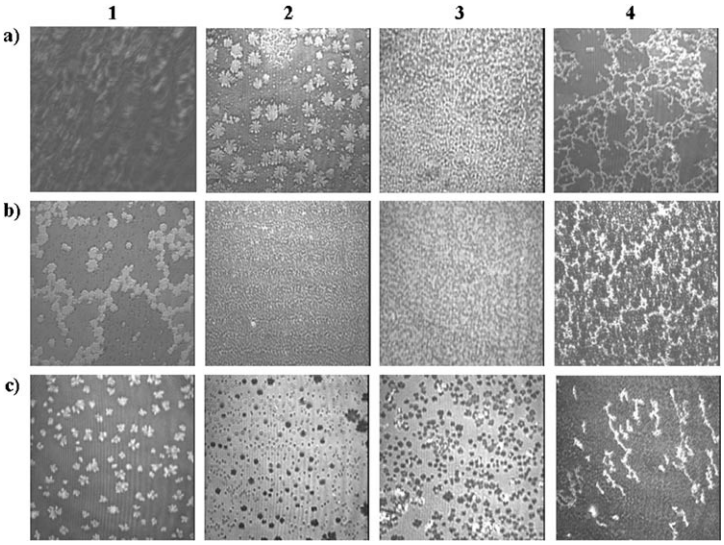

Figure 3. BAM images of Langmuir films. Panels 1 and 2: protonated NOA monolayer at 0 and 20 mN m^{-1}, panels 3 and 4: PNOA monolayer at 20 and 0 mN m^{-1}, with a) only sulfate, and additionally b) PVS, and c) CMC in the subphase. The images represent a 220 × 220 μm^2 area.

Optical-absorption spectra were recorded by using 24-layer LB films of PNOA polymerized at 20 mN m^{-1}; they

show a broad absorption with peaks at ~305, 445, and 565 nm[16] that can be assigned to a π–π* transition, a polaronic state with ammonium sites,[17] and pernigraniline form,[5] respectively. Negligible absorption above 625 nm indicates a low population of quinonoid structures.[13,17] PNOA is inferred to be in the fully protonated state with mostly benzenoid rings.

Monolayer films of PNOA deposited on mica by the Langmuir–Schafer method were examined by AFM. In the absence of polyelectrolytes (Figure 4a), a complex network

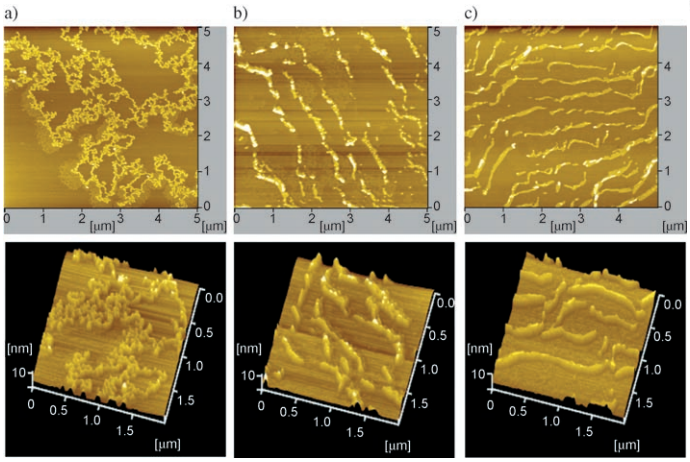

Figure 4. AFM topography images of monolayer Langmuir–Schafer films of PNOA fabricated with a) only sulfate, and additionally b) PVS, and c) CMC in the subphase. Top panel: 2D image ($5\times5\ \mu m^2$); bottom panel: 3D image ($2\ \mu m\times2\ \mu m\times10$ nm).

is observed with threads typically 3.5–4.0 nm high and 30–50 nm wide. Molecular modeling of the decamer unit of fully protonated PNOA shows the polyaniline chain with the hydrocarbon groups splayed out in a wedge shape; the cross-sectional dimensions are $\sim2.4\times2.6\ nm^2$ (Figure 5a). Based on this, the threads observed in the AFM image can be visualized as a monolayer of 12–20 PNOA chains with sulfate counterions assembled laterally forming a tapelike structure. Films fabricated in the presence of polyelectrolytes are dramatically different, showing enhanced alignment of extended polymer chains. Templating by amphiphiles is known to align arrays of conjugated polymers;[18] in the present case, the preorganized NOA amphiphiles possibly align the complexed polyelectrolytes, which in turn enforce orderly growth of the PNOA chains. Figure 4b and c show threads 4.0–4.5 nm high and 40–50 nm wide with PVS, and 3.8–4.2 nm high and 50–60 nm wide with CMC, respectively. Molecular modeling of the polyelectrolyte decamers (Figure 5b and c)[16] indicates cross-sectional dimensions of $\sim0.9\times0.9\ nm^2$ for PVS and $\sim0.7\times1.1\ nm^2$ for CMC; the latter dimensions are in good agreement with a previous model.[15] These estimates and the observed dimensions of the threads suggest plausible structures for the templated systems, consisting of PNOA chains on top of PVS and laterally placed alongside CMC. Figure 4b and c show that the

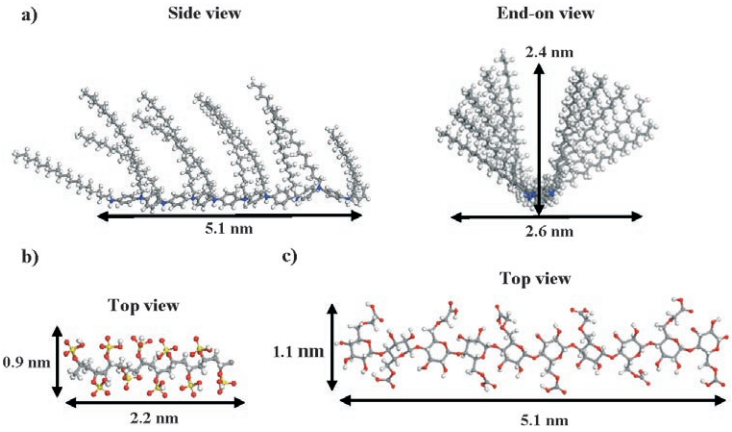

Figure 5. Optimized geometries of decamers of a) fully protonated PNOA, b) PVS, and c) CMC. The estimated average monomer length is 0.51, 0.22, and 0.51 nm, respectively. C (gray), H (white), N (blue), O (red), and S (yellow).

threads are segmented with lengths in the range 0.6–1.6 μm. Based on the average molecular weights of PVS and CMC (170000 and 90000, respectively) and the computed monomer lengths (0.22 and 0.51 nm, respectively), these polymer chains can be estimated to be ~0.2 μm long. Therefore the segment length appears to be built from 3–8 polyelectrolyte chains, along with the templated PNOA chain. If the average length of the PNOA chains is assumed to be ~1 μm, the computed monomer length of 0.51 nm suggests that the degree of polymerization is ~1960.

Conclusion

The present study has demonstrated that polyelectrolytes introduced in the subphase can have a profound impact on the morphology of Langmuir films, kinetics of polymerization at the air/water interface, and the formation of highly aligned polymer chains in the transferred ultrathin films. While the impact of PVS and CMC are beneficial, preliminary studies using poly(4-styrenesulfonate) indicate ambiguous effects—unique isotherms, absorption spectral shifts, and poor chain alignments—possibly due to additional and undesirable π-stacking interactions with polyaniline. Therefore, a judicious choice of the polyelectrolyte appears to be critical. Control of polymerization in monolayers at the air/water interface using the simple and efficient technique of polyelectrolyte complexation has significant implications for the fabrication of organized polymer assemblies for molecular electronics and photonics applications.

Experimental and Computational Section

Synthesis and characterization of NOA: The synthesis of NOA was carried out following Scheme 1. 1-Bromo-*n*-octadecane (1.0 g, 3 mmol) in toluene (20 mL) was added to a stirred solution of aniline (0.32 g, 3.3 mmol) in 30% aqueous NaOH containing a catalytic amount of

N,N,N,N-tetrabutylammonium bromide(PTC, phase-transfer catalyst). The reaction mixture was stirred at 70–80 °C for seven days. The toluene phase was washed with sodium chloride solution and evaporated. The resultant solid was purified by several recrystallizations from hexane. Yield: 0.82 g, 80 %; m.p. 50–52 °C; FT-IR (KBr): $\tilde{\nu}$ = 3396.9, 2916.6, 2847.2, 1604.9, 1510.4, 1468.0, 1315.6, 748.5, 690.6 cm^{-1}; ^1H NMR (200 MHz, $CDCl_3$, 25 °C, TMS): δ = 0.90 (t, J = 6.81 Hz, 3H), 1.27 (s, 30H), 1.60 (m, 2H), 3.10 (t, J = 6.89 Hz, 2H), 6.72 (m, 3H), 7.13 ppm (m, 2H) (amine proton is not observed); ^{13}C NMR (200 MHz, $CDCl_3$, 25 °C): δ = 148.6, 129.2, 117.0, 112.7, 44.0, 31.9, 29.7, 27.2, 22.7, 14.1 ppm.

Fabrication of Langmuir and LB/Langmuir–Schafer film: The LB experiments were carried out in a Nima Model 611M trough with a surface area of 30 × 10 cm^2. High-purity water (Millipore Milli Q) and chloroform (Uvasol grade, EMerck) were used for the subphase and spreading solution, respectively in all experiments; the volume of the subphase was ~220 mL. A quantity of 0.04 μmol of NOA was spread on the aqueous subphase containing sulfuric acid (0.10 M) or sulfuric acid and polyelectrolyte (~0.20 μmol based on the acid groups). The polyelectrolytes used were the potassium salt of PVS (average *MW* 170000) and the sodium salt of CMC (average *MW* 90000). Ammonium peroxydisulfate (typically 1.0 mL of a 1.7 M solution) was used as the oxidizing agent for polymerization. Reactions carried out at the air/water interface at 25 °C under constant pressure were monitored using the change in monolayer area (or barrier motion). Glass substrates for LB film deposition were cleaned with detergent, rinsed several times in water, and then sonicated in several batches of fresh water for 10–15 min each. A hydrophobic surface was prepared by exposing the slides to vapors of hexamethyldisilazane for 12 h. The LB film was deposited by vertical dipping of the substrate at a speed of 5 mm min^{-1}; transfer ratios were ~0.50. The Langmuir–Schafer film was transferred onto freshly cleaved mica by using a horizontal-dipping method.

Spectroscopy: Optical absorption spectra of multilayer LB films deposited on hydrophobic glass substrates by vertical dipping, were recorded on a Shimadzu model UV-3100 UV/Vis spectrometer. The absorption wavelength cut-off of the glass substrate is 270 nm.

Microscopy: The morphology of the Langmuir films at the air/water interface was observed by BAM. Images of the monolayer were recorded by using a Nanofilm Model BAM2Plus microscope. A 532 nm laser beam with a power of 20 mW was used. The monomer film was examined at different stages of compression. Following polymerization at a specific target pressure, the barriers were opened and closed again. Images were recorded throughout the whole procedure. The length scales of the images were corrected for the angle of incidence of the beam. Monolayers transferred to freshly cleaved mica plates by horizontal dipping, were imaged by using a Seiko Model SPA 400 atomic force microscope. All images presented were recorded in the dynamic-force (noncontact) mode; the tip had a force constant of 20 N m^{-1}. Line profiles were analyzed by using the software supplied by the microscope manufacturer.[16]

Molecular modeling: Computations were carried out by using the Accelrys MS Modeling 3.0.1 program. Monomer geometries were optimized and extended in steps to decamer units by using the "polymer build" option with geometry optimization at each stage carried out by using the Forcite module and Universal force field. Initial conformations were chosen as follows: PNOA with ammonium functionalities—the hydrophobic hydrocarbon chains oriented in the same direction to simulate their organization away from the aqueous subphase; PVS and CMC—the hydrophilic acid groups alternately on either side of the polymer backbone.

Acknowledgements

We thank the DST (NSTI program), New Delhi and UPE program of the UGC, New Delhi for financial and infrastructure support and Prof. M. Durga Prasad for fruitful discussions. MSC thanks CSIR, New Delhi for a senior research fellowship. Details of polymerization rates, absorption spectroscopy, line profile analysis of AFM images, and computed molecular structures are given in the Supporting Information.

[1] L. J. Kloeppner, R. S. Duran, *J. Am. Chem. Soc.* **1999**, *121*, 8108.
[2] K. Hong, M. F. Rubner, *Thin Solid Films* **1988**, *160*, 187.
[3] R. R. Bodalia, R. S. Duran, *J. Am. Chem. Soc.* **1993**, *115*, 11467.
[4] R. S. Duran, H. C. Zhou, *Thin Solid Films* **1992**, *210/211*, 356.
[5] L. J. Kloeppner, R. S. Duran, *Langmuir* **1998**, *14*, 6734.
[6] R. S. Duran, H. C. Zhou, *Polymer* **1992**, *210/211*, 4019.
[7] S. Sharma, M. S. Chandra, T. P. Radhakrishnan, *Langmuir* **2001**, *17*, 8118.
[8] a) M. S. Chandra, Y. Ogata, J. Kawamata, T. P. Radhakrishnan, *Langmuir* **2003**, *19*, 10124; b) M. S. Chandra, Y. Ogata, J. Kawamata, T. P. Radhakrishnan, *J. Nonlinear Opt. Phys. Mater.* **2004**, *13*, 347.
[9] M. S. Chandra, M. G. Krishna, H. Mimata, J. Kawamata, T. Nakamura, T. P. Radhakrishnan, *Adv. Mater.* **2005**, *17*, 1937.
[10] a) J. Liu, S. C. Yang, *J. Chem. Soc. Chem. Commun.* **1991**, 1529; b) M. Sudhakar, P. W. Stoecker, T. Viswanathan, *Recent Res. Dev. Polym. Sci.* **1998**, *2*, 173; c) W. Liu, A. L. Cholli, R. Nagarajan, J. Kumar, S. Tripathy, F. F. Bruno, L. Samuelson, *J. Am. Chem. Soc.* **1999**, *121*, 11345; d) R. Nagarajan, S. Tripathy, J. Kumar, F. F. Bruno, L. Samuelson, *Macromolecules* **2000**, *33*, 9542.
[11] S. Jayanty, G. K. Prasad, B. Sreedhar, T. P. Radhakrishnan, *Polymer* **2003**, *44*, 7265.
[12] H. Tachibana, Y. Yamanaka, H. Sakai, M. Abe, M. Matsumoto, *Thin Solid Films* **2001**, *382*, 257.
[13] a) A. Watanabe, K. Mori, A. Iwabuchi, Y. Iwasaki, Y. Nakamura, *Macromolecules* **1989**, *22*, 3521; b) J.-W. Chevalier, J.-Y. Bergeron, L. H. Dao, *Macromolecules* **1992**, *25*, 3325.
[14] J. Heesemann, *J. Am. Chem. Soc.* **1980**, *102*, 2167.
[15] J. Engelking, H. Menzel, *Thin Solid Films* **1998**, *327–329*, 90.
[16] See Supporting Information for details.
[17] B. Zhao, K. G. Neoh, E. T. Kang, K. L. Tan, *Chem. Mater.* **2000**, *12*, 1800.
[18] F. J. M. Hoeben, P. Jonkheijm, E. W. Meijer, A. P. H. Schenning, *Chem. Rev.* **2005**, *105*, 1491.

Received: July 17, 2005
Revised: October 19, 2005
Published online: February 2, 2006

